

Surface Phases in Binary Liquid Metal Alloys: An X-ray Study

Holger Tostmann,¹ Elaine DiMasi,² Oleg G. Shpyrko,¹
Peter S. Pershan,¹ Benjamin M. Ocko,² and Moshe Deutsch³

¹*Division of Applied Sciences and Department of Physics,
Harvard University, Cambridge MA 02138*

²*Department of Physics, Brookhaven National Laboratory, Upton NY 11973-5000*

³*Department of Physics, Bar-Ilan University, Ramat-Gan 52100, Israel*

Abstract

Surface sensitive x-ray scattering techniques with atomic scale resolution are employed to investigate the microscopic structure of the surface of three classes of liquid binary alloys: (i) Surface segregation in partly miscible binary alloys as predicted by the Gibbs adsorption rule is investigated for Ga-In. The first layer consists of a supercooled In monolayer and the bulk composition is reached after about two atomic diameters. (ii) The Ga-Bi system displays a wetting transition at a characteristic temperature $T_w \approx 220^\circ\text{C}$. The transition from a Bi monolayer on Ga below T_w to a thick Bi-rich wetting film above T_w is studied. (iii) The effect of attractive interactions between the two components of a binary alloy on the surface structure is investigated for two Hg-Au alloys.

PACS numbers: 61.25.Mv,61.10.-i

I. INTRODUCTION

Theoretical calculations and computer simulations indicate that the microscopic structure of the surface of liquid metals (LM) and alloys is considerably different from the surface structure of dielectric liquids and mixtures [1-3]. For liquid metals, the density profile normal to the surface has been predicted theoretically to show oscillations with a period of about one atomic diameter and extending a few atomic diameters into the bulk [2]. This layering normal to the surface has been confirmed experimentally for liquid Hg [4], Ga [5] and, most recently, In [6]. Surface induced layering in LM is due to the drastic changes in the interactions across the interface from short-ranged screened Coulomb interactions in the liquid phase to long-ranged van der Waals interactions in the gas phase. In dielectric liquids, on the other hand, van der Waals interactions prevail both in the liquid and in the gas phase and theory predicts a monotonic density profile [7].

Compared to elemental LM, binary LM alloys have an additional degree of freedom and it is possible to study the effect of the second component on surface induced layering. Moreover, binary mixtures are expected to exhibit a richer array of surface structures. In partly miscible mixtures for example, the lower surface tension component is expected to segregate at the surface as predicted by the Gibbs adsorption rule of thermodynamics [8]. For binary liquid metal alloys, computer simulations predict that the component that segregates at the liquid-vapor interface forms a nearly pure monolayer [9-11]. The adjacent layer on the bulk liquid side is slightly depleted of the surface-active component, and the bulk composition is reached at a distance of about two atomic diameters into the bulk. For simple dielectric mixtures on the other hand, theory predicts that the excess concentration of the segregating component falls smoothly with distance into the bulk over a range of several atomic diameters [8]. These predictions remain largely untested experimentally.

The bulk phase behavior of demixing leading to a miscibility gap with a critical consolute point induces a new class of surface phase transitions as predicted by Cahn in 1977 [12]. Based on scaling law arguments Cahn postulated that a phase transition from nonwetting of the two immiscible phases to complete wetting of one phase by the other necessarily occurs close to the critical consolute point. In this transition, a macroscopically thick wetting phase is formed intruding between the bulk liquid and the vapor phase (or an inert substrate). This is in contrast to the phenomenon of surface segregation that takes place on atomic length

scales. Experimental studies of such wetting phase transitions have been restricted mostly to binary dielectric mixtures [13]. Wetting and prewetting phase transitions have been observed only recently in fluid systems governed by screened Coulomb interactions [14], namely K-KCl [15], Ga-Pb [16] and Ga-Bi [17]. These experiments provide no direct microscopic information on the structure of the interface. By contrast, the study presented here probes the structure of the liquid interface with Å resolution using surface x-ray scattering techniques.

A characteristic feature of many well-known and technically important alloys is the formation of intermetallic phases in the solid state [18]. These phases include stoichiometric Laves phases, broad Hume-Rothery phases and semiconducting Zintl phases containing polyanions. This phase formation is due to attractive interactions between the two components. An interesting question is whether these attractive interactions affect the surface structure of liquid binary alloys.

In this paper, we will demonstrate how surface x-ray scattering techniques can be used to study LM alloys exhibiting different types of surface structure. In Sections 2 and 3 we review the x-ray scattering techniques and experimental details. In Section 4 we present three different alloy systems with increasing complexity of bulk phase behavior and surface structure: Ga-In, Ga-Bi and Hg-Au.

II. SURFACE X-RAY SCATTERING TECHNIQUES

X-rays are well suited to study the structure of the surface of liquids with atomic scale resolution. The large dynamic range in intensity required for such studies can be realized to advantage by synchrotron x-ray sources. In this section we describe the surface x-ray scattering techniques used in our studies to determine the structure normal to the surface and within the surface plane.

A. 2.1. Specular X-ray Reflectivity (XR):

X-ray reflectivity probes the structure normal to the interface. Here, the x-ray intensity is measured at the specular condition where incoming and outgoing angles α and β are equal and the azimuthal angle 2θ is zero (see Fig. 1). In this case, the scattering momentum

transfer, $\vec{q} = \vec{k}_{out} - \vec{k}_{in}$, is normal to the surface

$$|\vec{q}| = q_z = \frac{2\pi}{\lambda}(\sin \alpha + \sin \beta) = \frac{4\pi}{\lambda} \sin \alpha \quad (1)$$

where λ is the x-ray wavelength.

If the liquid surface is ideally flat and abruptly terminated (i.e. has a step function density profile), the reflectivity R is given by the Fresnel reflectivity R_f known from classical optics [19]. The reflectivity of a real surface will deviate from R_f . For example, height fluctuations produced by thermally excited capillary waves cause phase shifts in x-rays reflected from different points on the surface. Averaging over these phase variations gives rise to a Debye-Waller type factor, $\exp(-\sigma_{cw}^2 q_z^2)$, characterized by a capillary wave roughness σ_{cw} [6]. In addition, the density profile normal to the surface deviates from a step function, being oscillatory for elemental LM. For binary alloys displaying phase separation or phase transitions we expect further modification of the surface. Therefore, a surface structure factor Φ has to be taken into account [20]:

$$\Phi(q_z) = \frac{1}{\rho_\infty} \int_{-\infty}^{+\infty} \frac{d\langle\rho(z)\rangle}{dz} \exp(iq_z z) dz \quad (2)$$

with $\langle\rho(z)\rangle$ denoting the electron density average over a microscopic surface area on the atomic scale and ρ_∞ the bulk electron density. This factor is analogous to the bulk structure factor $S(\vec{q})$ which is the Fourier transform of the bulk electron density. The reflectivity from a real surface is then given by:

$$R(q_z) = R_f \exp(-\sigma_{cw}^2 q_z^2) |\Phi(q_z)|^2. \quad (3)$$

It is not possible to directly invert the measured reflectivity $R(q_z)$ to the density profile normal to the surface due to the loss of phase information. Rather, the common practice is the construction of a physically plausible model for the density profile which is then inserted in eq.(2) and fitted to the measured reflectivity [6,21].

B. Grazing Incidence Diffraction (GID):

GID probes the in-plane structure of the surface. The in-plane momentum transfer q_{xy} is probed by varying the azimuthal angle 2θ (see Fig. 1). This geometry is surface sensitive if the incident angle α is kept below the critical angle for total external reflection α_{crit} thereby

limiting the x-ray penetration depth to $\simeq 50\text{\AA}$ and minimizing the background from bulk scattering [22,23]. The GID surface in-plane structure can be directly compared to the bulk liquid structure by making similar measurements for $\alpha > \alpha_c$.

III. EXPERIMENTAL

It is essential to establish a clean oxide free liquid alloy surface since even microscopic impurities significantly change the x-ray reflectivity [24]. We use slightly different methods to prepare the three alloys presented in this paper. The eutectic Ga-In alloy is prepared in a High Vacuum chamber using in situ glow-discharge to clean the sample [21]. The sample is transferred into the x-ray UHV chamber, melted and cleaned by Ar ion sputtering.

The Ga-Bi alloy is prepared as follows. Bi is melted under UHV conditions and any residual oxide is evaporated by heating the Bi to about 600°C . After the Bi is transferred into an Ar glove box, liquid Ga is added so that the mole fraction of Bi is $x_{Bi} \approx 0.3$. This value is chosen to correspond to the concentration of the bulk solution at the critical point of 265°C . The sample is then frozen and transferred to the x-ray UHV chamber. The chamber is baked out and the liquid surface sputter cleaned.

The preparation of the Hg-Au alloy is quite different since the high vapor pressure of Hg is not compatible with UHV conditions. Quadruple distilled Hg and Au powder are mixed in a glove box and transferred to a stainless steel reservoir attached to a valve with a filling capillary. This container is attached to a UHV chamber with the valve closed. This chamber is then subjected to a standard UHV bakeout to remove oxygen and water, after which the valve is opened and the Hg-Au alloy is poured into the sample pan. Due to the low oxygen partial pressure in the chamber, residual oxide is instable and disappears from the surface within a couple of hours.

The sample chamber is placed on an active vibration isolation table that effectively quenches all mechanically induced vibrations [6]. The experiments have been performed at the beamlines X22B and X25 at the National Synchrotron Light Source at Brookhaven National Laboratory. The x-ray energies are 19keV and 10keV at X25 and X22B respectively. A discussion of the liquid surface spectrometer can be found elsewhere [21].

IV. RESULTS AND DISCUSSION

A. Surface Segregation in Ga-In

As an example of a simple miscible alloy with a eutectic point we have studied the Ga-In (16.5% In) system [21]. The Fresnel-normalized reflectivity is shown in Fig. 2 (filled squares). The data have been recorded at room temperature and are compared to the normalized reflectivity from elemental Ga (open squares) at the same temperature. The most pronounced feature of the Ga reflectivity is the quasi-Bragg peak at 2.4 \AA^{-1} that indicates the presence of surface induced layering [5]. This layering peak is present in the Ga-In alloy as well, although slightly suppressed. The peak position is centered at a smaller value of q_z compared to Ga indicating a larger layer spacing, as expected for a larger In atom. The second pronounced difference between the Ga-In and the Ga reflectivity is the observation that the reflectivity from Ga-In is about 30% higher than the Fresnel reflectivity of an ideal Ga-In surface at intermediate values for q_z . This can only be understood if a higher density adlayer exists at the surface. The measured x-ray reflectivity is consistent with the segregation of a 94% In monolayer on top of the Ga-In eutectic. The presence of the In monolayer increases the reflected x-ray intensity at intermediate q_z due to the higher electron density of In but has a less pronounced effect at larger q_z values where the reflectivity is dominated by the Ga layering peak. The density profile that fits the measured XR can be modeled by a single Gaussian for the In segregation layer plus a semi-infinite sum of Gaussians for the Ga-In eutectic with half widths that increase with distance from the surface, representing the decay of the layering with increasing distance from the surface [21]. The best fit of this model to the data results in a density profile normal to the surface that shows the segregation of an In monolayer with a 2.6 \AA spacing between the In monolayer and the underlying eutectic layer. This fit is represented by the solid line in Fig. 2.

These results provide new information about the surface structure of miscible LM alloys. The constituents of this alloy have similar size and the same valency. The Ga-In interactions are comparable to the Ga-Ga and the In-In interactions. As a consequence, Ga-In is close to being an ideal mixture, for which surface segregation of the lower surface tension component is predicted. Our measurements show that this segregation is actually confined to a single monolayer. An arguably more interesting issue is the interplay between surface segregation

and surface induced layering. Our measurements show that layering persists, with the In monolayer comprising the outermost layer. Similar conclusions were reached by recent Quantum Molecular Dynamics simulations [25].

B. Wetting phase transition in Ga-Bi

The Ga-Bi system is an example of an alloy with a miscibility gap. Below the monotectic temperature, $T_{mono} = 222^\circ\text{C}$, a Ga rich liquid coexists with a solid Bi phase. (see [26] for a full description of the phase diagram). However, due to its lower surface energy a Bi monolayer is expected to segregate at the surface of the Ga rich liquid. The wetting phase transition that is predicted for all binary mixtures with critical demixing [12] occurs at a characteristic wetting temperature T_w below the critical temperature T_{crit} [27,28]. Optical studies show that T_w coincides with the monotectic temperature for Ga-Bi [14,17]. Above T_w , a macroscopically thick Bi rich phase is expected to completely wet the lighter Ga rich phase in defiance of gravity. The Bi concentration in the Ga rich phase increases with increasing temperature as long as the liquid coexists with the solid Bi phase.

The normalized x-ray reflectivity spectra, $R/R_{f,Ga}$, for Ga-Bi at 35°C and 95°C are shown in Fig. 3 versus q_z^2 . At the lowest values of q_z , the normalized reflectivity approaches the reflectivity of an ideal Ga surface given by the Fresnel Law of Optics. At values of q_z close to the critical q-vector $q_{crit} = 4\pi/\lambda \sin \alpha_{crit}$, the reflectivity is not particularly sensitive to the structure or roughness of the surface (see eq.(3)) and is simply related to the electron density within $\approx 20 \text{ \AA}$ of the surface. The fact that the reflectivity approaches the Fresnel reflectivity given by the Ga electron density implies that the higher density Bi can not be more than a few monolayers thick. With increasing q_z , the normalized reflectivity first increases and reaches a maximum at about $q_z \approx 1 \text{ \AA}^{-1}$. The variation of $R/R_{f,Ga}$ with q_z , is similar to that observed by Lei et al. [10], corresponding to the thickness of a single atomic layer, again suggesting that only the top layer has a sizeable bismuth concentration. Compared to the Ga-In alloy discussed above, this variation is much more pronounced. This results from the 30% higher electron density of bismuth compared with gallium, and only a 5% higher density for indium. The behavior of the same alloy at 260°C is markedly different. Here, the reflectivity starts out at $R/R_{f,Ga} \approx 2$ and falls off monotonically with q_z , a behavior consistent with a thick Bi rich layer terminating the metal/vapor interface above T_w .

The reflectivity below $T_w \approx 220^\circ\text{C}$ has been analyzed in terms of a density profile similar to the one which describes the Ga-In data [21]. The best fits, the solid lines in Fig. 3, provide an excellent description of the data. The corresponding local density profile, shown in Fig. 4 after removing the temperature dependent capillary wave roughness factor, exhibits a top-layer density which is about 1.5 times higher than the Ga bulk liquid density and is consistent with the formation of a complete Bi monolayer. The $3.6 \pm 0.2 \text{ \AA}$ layer spacing between the monolayer and the adjacent Ga layer (obtained from the fits) is much larger than the $2.5 \pm 0.1 \text{ \AA}$ layer spacing obtained in liquid gallium. This also supports the conclusion of a top layer with a much larger atomic diameter. In addition, the 4.3 \AA exponential decay length of the layering amplitude is significantly smaller than the 5.5 \AA decay length obtained for pure liquid Ga [5]. The suppression of the layering in the presence of either a bismuth or indium monolayer is much more apparent in the case of bismuth (compare Fig. 3 to Fig. 2). A likely explanation is the larger size difference in Ga-Bi (the Bi diameter is 30% larger than that of Ga) compared to Ga-In (In is 15% larger than Ga). As demonstrated by the solid lines, the layering model which describes the 35°C reflectivity profile also agrees closely with the 95°C profile, without a discernible change in the parameters of the density profile, except for the value of σ_{cw} , which is scaled, using capillary wave theory, to correspond to the higher temperature (see eq.(3)).

This picture of a Bi monolayer segregating on top of the Ga rich bulk phase is supported by GID experiments which probe the in-plane structure of the surface (see Fig. 5). The solid line shows the in-plane liquid structure factor measured for $\alpha > \alpha_{crit}$ where the x-rays penetrate the bulk to a depth $> 1000 \text{ \AA}$. The broad peak at $q_{xy} \approx 2.5 \text{ \AA}^{-1}$ and the shoulder on the high-angle side of the peak agree with bulk liquid Ga structure factor [29]. There is no evidence for a peak or shoulder at the position corresponding to the first peak of the Bi liquid structure factor at $q_{xy} \approx 2.2 \text{ \AA}^{-1}$. The bulk scattering completely masks the weak scattering from the bismuth monolayer due to the large penetration depth of x-rays. The surface sensitivity is drastically enhanced by keeping the incoming angle α below the critical angle for total external reflection (0.14° for Ga). As the x-rays now penetrate only to a depth $< 50 \text{ \AA}$, the first peak of the Bi liquid structure factor is clearly visible at $q_{xy} \approx 2.2 \text{ \AA}^{-1}$ (open triangles in Fig. 5). Still, since the Bi layer is only a single monolayer thick, the contribution from the underlying Ga is larger than that of the Bi, as seen from the Bi being only a shoulder on the Ga structure factor peak in Fig. 5.

While the XR results at 35° C and 95° C are consistent with a real space model where the Bi is segregated only in the top atomic layer, at temperatures above 220° C, corresponding to a Bi mole fraction of about 0.08, this model no longer describes the data. The ratio $R/R_{f,Ga}$ for the reflectivity taken at 260° C close to the critical wavevector for Ga is approximately twice as large as the same ratio taken at 35° C and 95° C. The dashed horizontal line, shown in the inset to Fig. 3, represents the theoretical Fresnel-normalized reflectivity curve for bulk Bi ($R/R_{f,Bi} \approx 2 \times R/R_{f,Ga}$). This curve agrees well with the 260° data at small q_z where the surface roughness contribution is minimal, and clearly supports the conclusion of a thick Bi-rich surface layer. Such a thick wetting layer has been proposed on the basis of previous optical experiments [14,17]. These findings are also supported by GID experiments above 220° C which show a pronounced increase in the intensity of the Bi structure factor relative to the Ga structure factor [30].

C. Pair formation in Hg-Au

Our x-ray reflectivity measurements of dilute liquid Hg-Au alloys demonstrate that dramatic differences in surface structure can be induced by very small changes in concentration. Fig. 6(a) compares the reflectivity of Hg with that of a solution of 0.06at% Au in Hg. This composition is approximately half of the reported solubility limit for Au in Hg at room temperature [26]. For pure Hg, the surface layering peak at $q_z = 2.2 \text{ \AA}$ is much more prominent close to its melting point at -40°C than at room temperature [31]. This difference arises primarily from increased roughening of the surface due to thermally excited capillary waves with increasing temperatures. The presence of 0.06at% Au sharply suppresses the surface induced layering of Hg, as shown by the substantial attenuation of the layering peak. The temperature dependence in both systems suggests that at this concentration, the suppression of the surface layering by the Au has a small dependence on temperature in comparison to the effect of capillary waves.

Increasing the Au concentration to 0.13at% yields a qualitatively different behavior as shown in Fig. 6(b). At room temperature, layering is suppressed to a similar extent in both alloys. However, upon lowering the temperature of the 0.13at% solution to -30°C , a deep minimum appears at $q_z = 1.4 \text{ \AA}^{-1}$. This minimum is produced by destructive interference between x-rays reflecting from layers of different density near the surface, implying that

one or more phases have formed that are different from the composition of the bulk. We find significant hysteresis of the reflectivity under temperature cycling. In particular, on returning to room temperature and cooling again, the low temperature minimum is much less deep than that observed previously, and saturates at this higher value even when the sample is supercooled to about -70°C . This pronounced effect has been reproduced and in the absence of detailed modeling we can only speculate about its origin. As opposed to Ga-In and Ga-Bi, the interactions between Hg and Au are attractive leading to intermetallic phase formation in the solid state with Au_2Hg being the best known phase [26]. Several other phases have been reported that are only stable below -39°C [26]. It is known from x-ray studies on FeCo (001) [32] and Cu_3Au (001) [33] surfaces, that this pair formation gives rise to mesoscopic surface segregation profiles in the solid state. As soon as one component segregates at the surface, it is energetically favorable for the next layer to consist entirely of the other component due to the pronounced attractive interactions. It is conceivable that a similar mechanism prevails in liquid Hg-Au. An alternating or more complicated segregation profile would destroy the Hg layering even more effectively than the segregation of a monolayer in Ga-In or Ga-Bi and is consistent with our experimental findings that a small amount of Au completely suppresses the otherwise very pronounced Hg layering peak even at low temperatures.

V. ACKNOWLEDGEMENTS

This work has been supported by the U.S. Department of Energy Grant No. DE-FG02-88-ER45379, the National Science Foundation Grant No. DMR-94-00396 and the U.S.–Israel Binational Science Foundation, Jerusalem. Brookhaven National Laboratory is supported by U.S. DOE Contract No. DE-AC02-98CH10886. HT acknowledges support from the Deutsche Forschungsgemeinschaft.

References

- [1] M.Iwamatsu and S.K.Lai, *J.Phys.:Condens.Matter* *4*, 6039 (1992).
- [2] J.G.Harris, J.Gryko and S.A.Rice, *J.Chem.Phys.* *87*, 3069 (1987).

- [3] R.Evans and M.Hasegawa, *J.Phys.C:Solid State Phys.* *14*, 5225 (1981).
- [4] O.M.Magnussen, B.M.Ocko, M.J.Regan, K.Penanen, P.S.Pershan and M.Deutsch, *Phys.Rev.Lett.* *74*, 4444 (1995).
- [5] M.J.Regan, E.H.Kawamoto, S.Lee, P.S.Pershan, N.Maskil, M.Deutsch, O.M.Magnussen, B.M.Ocko and L.E.Berman, *Phys.Rev.Lett.* *75*, 2498 (1995).
- [6] H.Tostmann, E.Dimasi, P.S.Pershan, B.M.Ocko, O.G.Shpyrko and M.Deutsch, submitted (1998).
- [7] G.A.Chapella et al., *J.Soc.FaradayII* *73*, 1133 (1977).
- [8] J.S.Rowlinson and B.Widom, *Molecular Theory of Capillarity*, Clarendon, Oxford, 1982.
- [9] J.G.Harris and S.A.Rice, *J.Chem.Phys.* *86*, 7531 (1987).
- [10] N.Lei, Z.Huang and S.A.Rice, *J.Chem.Phys.* *104*, 4802 (1996).
- [11] S.A.Rice, M.Zhao and D.Chekmarev, submitted (1998).
- [12] J.W.Cahn, *J.Chem.Phys* *66*, 3667 (1977).
- [13] M.Schick in: *Liquids at Interfaces (Proceedings Les Houches Summer School, Session XL)*, ed. by J.Charvolin, J.F.Joanny and J.Zinn-Justin, North-Holland, Amsterdam, 1990.
- [14] W.Freyland and D.Nattland, *Ber.Bunsenges.Phys.Chem.* *102*, 1 (1998).
- [15] H.Tostmann, D.Nattland and W.Freyland, *J.Chem.Phys.* *104*, 8777 (1996).

- [16] D.Chatain and P.Wynblatt, *Surf.Sci.* *345*, 85 (1996).
- [17] D.Nattland, S.C.Müller, P.D.Poh and W.Freyland, *J.Non-Cryst. Solids* *205–207*, 772 (1996).
- [18] W.B.Pearson, *The Crystal Chemistry and Physics of Metals and Alloys*, Wiley, New York, 1972.
- [19] J.Als-Nielsen in: *Structure and Dynamics of Surfaces*, *Topics in Current Physics* 43, ed. by W.Schommers and P.von Blanckenhagen, Springer, Heidelberg, 1987.
- [20] P.S.Pershan and J.Als-Nielsen, *Phys.Rev.Lett.* *52*,759 (1984).
- [21] M.J.Regan et al., *Phys.Rev.B* *55*,15874 (1997).
- [22] P.Eisenberger, W.C.Marra, *Phys.Rev.Lett.* *46*, 1081 (1981).
- [23] H.Dosch, *Critical Phenomena at Surfaces and Interfaces*, Springer Tracts in Modern Physics, Vol. 126, Springer, Heidelberg, 1987.
- [24] M.J.Regan, H.Tostmann, P.S.Pershan, O.M.Magnussen, E.DiMasi, B.M.Ocko and M.Deutsch, *Phys.Rev.B* *55*, 10786 (1997).
- [25] S.A.Rice and M.Zhao, submitted (1998).
- [26] T.B.Massalski et al. (eds.), *Binary Alloy Phase Diagrams*, ASM International, Materials Park, Ohio, 1990.
- [27] S.Dietrich, *Wetting Phenomena*, in: *Phase Transitions and Critical Phenomena*, Vol. 12, ed. by C.Domb and J.Lebowitz, Academic Press, London, 1986.
- [28] S.Dietrich, G.Findenegg and W.Freyland (eds.), *Phase Transitions at Interfaces*

(Proceedings Bunsen Discussion Meeting), Ber.Bunsenges.Phys.Chem. 98 (1994).

[29] A.H.Narten, J.Chem.Phys. 56, 1185 (1972).

[30] H.Tostmann, E.DiMasi,O.G.Shpyrko, P.S.Pershan, B.M.Ocko, and M.Deutsch, in preparation (1998).

[31] E.DiMasi, H.Tostmann, B.M.Ocko, P.S.Pershan and M.Deutsch, in preparation (1998).

[32] S.Krimmel et al., Phys.Rev.Lett. 78, 3880 (1997).

[33] H.Reichert, P.Eng, H.Dosch and I.K.Robinson, Phys.Rev.Lett. 74, 2006 (1995).

Figure Captions

Fig. 1 Sketch of the geometry of x-ray scattering from the liquid surface with α and β denoting incoming and outgoing angle, the incoming and outgoing wavevector k_{in} and k_{out} respectively and the azimuthal angle 2θ . The momentum transfer q has an in-plane component q_{xy} and a surface-normal component q_z .

Fig. 2 X-ray reflectivity from liquid Ga and liquid Ga-In (16.5% In) at 25° C. The broken line represents the fit of the model described in the text to the measured reflectivity from liquid Ga. The solid line represents the fit of the same model with one additional high density adlayer to the measured reflectivity from the liquid Ga-In eutectic.

Fig. 3 X-ray reflectivity from Ga-Bi for three different temperatures. The solid lines show the fit of the data to a simple surface segregation model with one Bi monolayer on top of the Ga rich bulk phase. The difference between the 35° C and the 95° C data is due to the increased roughness at higher temperatures. The 260° C data cannot be fitted by this model. The inset shows the principal difference in surface structure between the 35° C and the 260° C data, indicating a wetting phase transition.

Fig. 4 Comparison of the intrinsic or local real space density profiles (thermal broadening removed) for Ga-Bi at two different temperatures as well as for elemental Ga. The density is normalized to the bulk density of liquid Ga. The zero position in z is arbitrarily assigned to the center of the first Ga layering peak.

Fig. 5 Grazing Incidence Diffraction from Ga-Bi at 35° C. The solid line shows the in-plane structure averaged over the penetration depth of x-rays away from the critical angle for total external reflection (about 1000 Å). The open triangles show the diffraction peak obtained for $\alpha < \alpha_{crit}$ ($\alpha_{crit} = 0.14^\circ$ for Ga at $\lambda = 0.653\text{Å}$) thus probing the surface region evanescently.

Fig. 6 (a) X-ray reflectivity of Hg and Hg/0.06at%Au normalized to the Fresnel reflectivity of Hg. (b) Normalized reflectivity of a Hg/0.13% alloy.

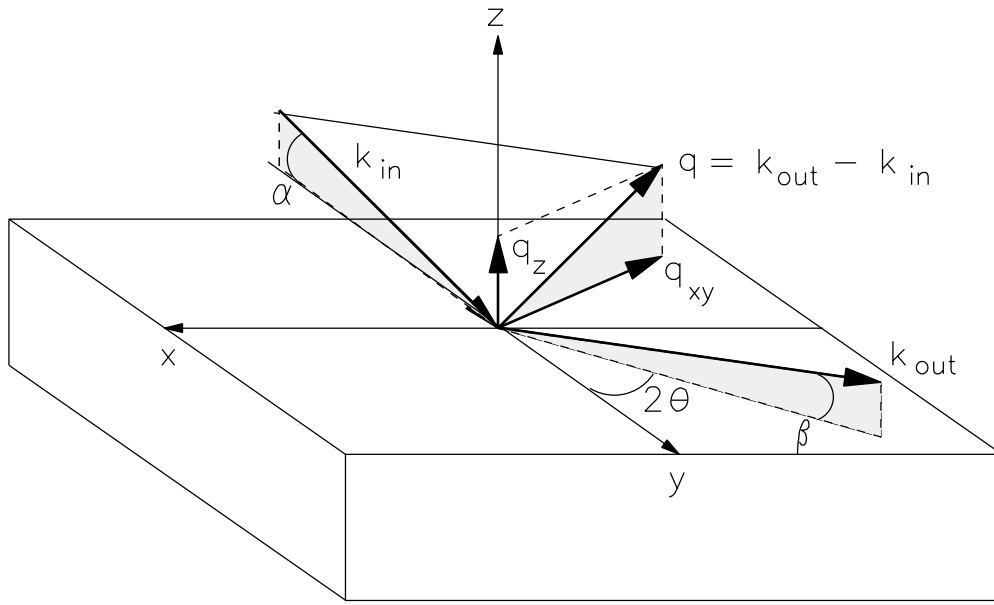


Fig. 1 Tostman et al.

